



CFD Investigation of the Effect of Vibration Direction on the Heat Transfer Enhancement of Heat Sink

Ambagaha Hewage Dona Kalpani Rasangika¹, Mohammad Shakir Nasif^{1,*}, William Pao¹, Rafat Al-Waked²

¹ Department of Mechanical Engineering, Universiti Teknologi PETRONAS, Seri Iskandar 32610 Perak, Malaysia

² Department of Mechanical and Maintenance Engineering, German Jordanian University, 11180 Amman, Jordan

ARTICLE INFO

Article history:

Received 17 February 2023

Received in revised form 15 March 2023

Accepted 16 April 2023

Available online 1 October 2023

Keywords:

Heat Transfer Enhancement; Vertical Vibration; Horizontal Vibration; Sinusoidal; Square

ABSTRACT

The application of vibration on a heated surface is found to be one of the promising cooling methods. Previous studies found that the thermal performance of the heated body depends on the vibrational characteristics and wave shape. However, for heat sinks, the direction of the vibration for different vibrational wave shapes has not been investigated, which may influence cooling. Thus, the current study conducted a numerical investigation to study the effect of the vibration direction of sinusoidal and square wave shaped vibration on the conventional heat sink and validated it against experimental results with a maximum deviation of 2.4%. The study is conducted with a range of frequencies and peak-to-peak amplitude of 0-80 Hz and 0-0.005 m under the square and sinusoidal wave shapes. It was found that the Nusselt number increases with higher frequencies ($f > 40$ Hz), and amplitudes and enhancement in Nusselt values are more dominant with square wave shapes. At the vibration frequency and peak-to-peak amplitude of 80 Hz and 0.005 m, a maximum of 9.3 % and 7.2 % enhancement in the Nusselt number is recorded with square and sinusoidal vibration, respectively. Moreover, the result of the current study is compared with the published work, and it was concluded that the effect of vibration on heat transfer is superior to horizontal vibration in comparison with vertical vibration by 7% and 3.2% under square and sinusoidal wave shaped vibrations, respectively.

1. Introduction

The continuous development of the electronic industry and miniaturization of electronic components has led to increased circuit packaging densities, resulting in a higher generation of heat flux. Consequently, designing a high-power dissipation mechanism in limited space has become a primary design effort for electronic system designers to improve the reliability and functionality of components. Thus, several promising cooling mechanisms have been invented. Among those cooling methods, free and forced convection are considered the most common electronic cooling method

* Corresponding author.

E-mail address: mohammad.nasif@utp.edu.my (Mohammad Shakir Nasif)

by several studies [1-4]. Furthermore, as investigated by researchers, further enhancement is achieved using extended surfaces like fins, which helps decrease the thermal resistance [5].

However, when convection occurs, as mentioned by several studies [6,7], the thermal boundary layer is generated on either side of extended surfaces or heat sinks, and it limits cooling capacity by hindering the heat transfer between a heated body and adjacent fluid. On the other hand, reducing or disturbing this induced thermal boundary layer can lead to a reduction in thermal resistance, thus enhancing convective heat transfer. Therefore, researchers invented different techniques incorporated with a convective cooling system to disturb the thermal boundary layer formation. Generally, these methods can be classified into passive and active.

As explained by Kannan and Kamatchi [8], passive techniques to improve heat transfer involve changing the physical properties of the heated surface or fluid without using external energy. Application of surface coatings at the micron scale of the heated surface, hydrodynamic cavitation, and turbulators or mixing promoters are some of the common passive methods investigated by several authors [9-15]. These methods are incorporated with the convection of heat sinks, used to disturb the thermal boundary layer formulation by improving the fluid mixing. Moreover, using nanofluid to obtain elevated thermal performance is also a popular passive cooling technology among researchers [16-19]. However, as mentioned by several researchers [15,20], passive techniques alone are insufficient to meet the growing heat dissipation demand of electronic systems, making active techniques necessary. Active methods use the external power to increase the heat transfer coefficient and disturb the thermal boundary layer by applying the magnetic or electrical field, air jets, and spray inspired by researchers [20-25].

With the increasing demand for market development of electronic systems, modern electronic devices move towards miniaturization, thinness, and lightness. Therefore, the challenging tasks of electronic cooling methods are not only being highly efficient in heat dissipation but also coherent with the trend of miniaturization in modern electronic systems. Thus, disturbing the thermal boundary layer through external vibration to obtain enhanced heat dissipation has been a promising electronic cooling method since this efficient cooling effect can be utilized to the miniature of the cooling system.

Above two decades, most researchers focused on heat transfer enhancement of oscillating cylinders, such as horizontal oscillations by Shalaby *et al.*, [26], vertical oscillation by Pottebaum and Gharib [27], Seenivasan and Ramachandran [28], Gau *et al.*, [29] and Dawood *et al.*, [30]. It is noteworthy to mention that those studies found notable heat transfer enhancement by the application of external vibration. Karanth *et al.*, [31] investigated heat transfer with horizontal and vertical oscillating cylinders and observed a significant enhancement in thermal performance. However, the authors did not comprehensively discuss the vibration direction effect on the thermal performance of oscillating cylinders. In their numerical studies, Shokouhmand *et al.*, [32,33] investigated the vertically and horizontally oscillating 2D cylinders. These studies indicate that horizontal vibration can potentially increase heat transfer further compared to vertical vibration.

With the increasing power generation and miniaturization trend of electronic systems, researchers have been interested in applying vibration on fins and heat sinks within the last two decades. Gururatana and Li [34] and Rahman and Tafti [35] investigated the horizontal and vertical vibration of 2D fin, respectively, and observed the higher heat transfer enhancement and highest vibrational characteristics. Furthermore, Najim *et al.*, [36] investigated the heat transfer enhancement of a vertically oscillating heat sink, and a significant enhancement in heat transfer was observed with higher frequencies.

Although all the above studies have only focused on the thermal performance of an oscillating heated body under the influence of sinusoidal vibration, Rasangika *et al.*, [37] investigated the

thermal efficiency of the horizontally oscillating heat sink under sinusoidal and square wave shapes, and they observed a maximum of 25% higher heat transfer enhancement with square wave shaped vibration. Moreover, it was revealed that square wave-shaped vibration has a prominent effect on heat transfer enhancement over sinusoidal vibration at each vibration level. However, the study only focused on horizontal vibration. The vibration of the heated body induces a turbulence effect in the fluid flow, which helps to disturb the thermal boundary layer, thus enhancing the convective heat transfer. However, as mentioned in studies [32,33], this turbulence effect is not only associated with vibrational characteristics and wave shape; it may also be influenced by the direction of the external vibration. Thus, for heat sinks, it is essential to compare the impact of both horizontal and vertical vibration on the thermal efficiency of a conventional heat sink with both sinusoidal and square wave shapes. Therefore, the present study aims to investigate the influence of vibration direction on the forced convective heat transfer of a conventional heat sink that vibrates with square and sinusoidal vibrations over a range of vibration frequencies and amplitudes. Moreover, this paper compares the thermal performance of a vertically vibrating heat sink with the results of Rasangika *et al.*, [37] under a horizontally vibrating heat sink. Therefore, the three-dimensional numerical model, similar to the study of Rasangika *et al.*, [37], simulated using ANSYS/ FLUENT to obtain the heat transfer enhancement under vertical vibration and validate against the experimental results.

2. Experimental Method

The experimental setup is designed to obtain the vertical vibration of the heat sink. The schematic diagram of the experimental set-up is shown in Figure 1.

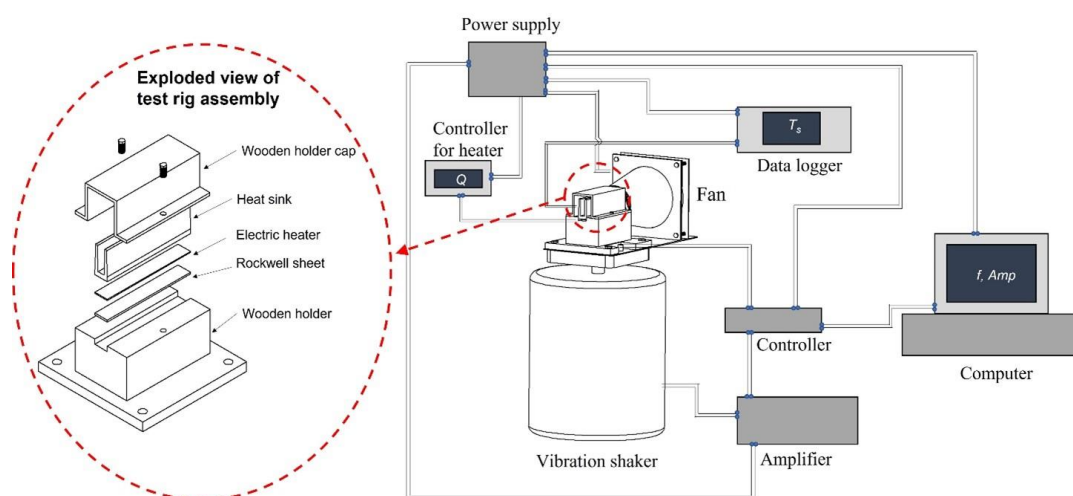


Fig. 1. Schematic diagram of the experimental setup

The heat sink is made of Aluminium (Alloy 6061), and the dimensions of the heat sink are shown in Figure 3(a). As illustrated in Figure 1, the heat sink is mounted using the wooden holder consisting of a groove with dimensions of 0.016m wide, 0.095m long, and 0.005m deep. The Rockwool insulation sheet is placed on the base of the groove to minimize heat loss. The variable capacity digital heater is attached to the base of the heat sink and placed in the groove over the insulation sheet. The test rig is tightly held within the wooden holder and is covered by the wooden holder cap using tight bolts on the wooden holder. The wooden holder is mounted to the horizontal frame. The conical air passage, which works as a guide to supply the uniform air stream to the heat sink and variable speed fan, was vertically installed at one end of the frame. The frame is mounted vertically on the vibration shaker platform, which receives its vertical sinusoidal vibration from the vibration shaker

(M060-CE; IMV). The required sinusoidal frequency and acceleration are given to the controller of the shaker, and the accelerometer connected to the shaker platform is used to obtain the feedback for the closed-loop system. In order to measure the temperature of the channel wall, the K-type of eight thermocouples is embedded beneath the channel wall in two fins at equal distance locations along fin length. A temperature data logger (AT4524; Applent) was used to record the temperature data obtained by the thermocouples. An uncertainty analysis has been performed to obtain the experimental error.

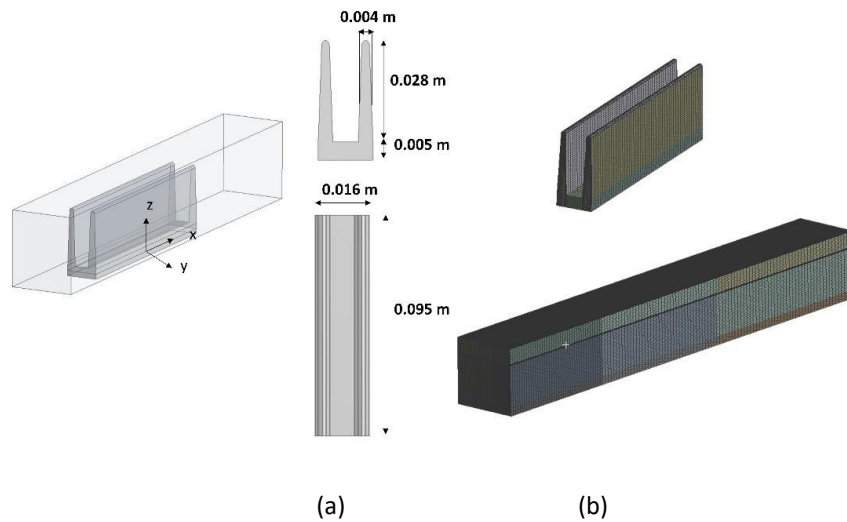


Fig. 2. (a) Geometry of heat sink with dimensions (b) Computational domain with mesh

Certain parameters are defined to determine the enhancement of the thermal performance of the heat sink with and without vibration conditions. The heat generated by the Digital heater is transferred to the heat sink by conduction, and it dissipates to surrounded air by convection. It is assumed the heat dissipated by radiation and heat loss to the surrounding are negligible. Thus, the convection heat transfer coefficient (h) can be specified as follows:

$$h = \frac{Q}{A_f(T_f - T_{in})} \quad (1)$$

Here Q , A_f , T_f , and T_{in} represent the heat transfer rate, heat transfer surface area, and the average temperature recorded by the thermocouples and inlet flow temperature, respectively. The temperature measurements were obtained when its reading remained constant within $\pm 0.1^\circ\text{C}$ over 3 minutes. For the calculations of other parameters, the fluid properties are determined at the average air temperature of the inlet and outlet. The heat transfer enhancement of the vibrating heat sink is evaluated by using the Nusselt number, which is denoted by:

$$Nu = \frac{h W}{k_f} \quad (2)$$

Here W represents the width of the channel area between two fins, and k_f is the thermal conductivity of air. The air velocity is measured using a digital anemometer (ST730; SENTRY) just after leaving the wooden cap. Based on averaged velocity (U), the Reynolds number is calculated, which is given by:

$$Re = \frac{\rho UW}{\mu} \quad (3)$$

Here ρ and μ are the density and dynamic viscosity of the fluid.

3. Simulation Method

3.1 Geometry, Boundary Conditions and Governing Equations

The simulation domain of the current study is shown in Figure 3. The bottom surface of the heat sink is assigned as a heat source with a constant heat flux of 6250 W/m². A consistent inlet velocity in the x-direction is used, with a Reynolds number of 1000 at a temperature of 25°C. The vibration is applied in the Z direction of the heat sink. In order to obtain the vibration in ANSYS/FLUENT software, UDF codes are developed for each vibration type using the displacement functions, which are given by Eq. (4) and Eq. (5).

$$Z(t) = A \sin(2\pi ft) \quad (4)$$

$$Z(t) = \frac{4A}{\pi} \sum_{n=1,3,5..}^N \frac{1}{n} \sin(2\pi nft) \quad (5)$$

Here $Z(t)$ represents the heat sink vertical displacement at any time, and f , A and t represent the vibrational frequency, amplitude, and time, respectively.

In the current study, the governing equations are based on the conservation laws of Mass, Momentum, and Energy. It is assumed that the flow is a laminar, incompressible, ideal gas with constant thermophysical characteristics. The body forces are assumed to be negligible, and no-slip conditions are subjected to the interface between solid and fluid. Thus, based on the study of Rasangika *et al.*, [38], the governing equations of the study can be presented below :

Continuity equation:

$$\frac{\partial v_i}{\partial x_i} = 0 \quad (6)$$

Momentum equations:

$$\rho \frac{\partial(v_i)}{\partial t} + \rho \frac{\partial(v_i v_j)}{\partial x_j} = -\frac{\partial P}{\partial x_i} + \mu \frac{\partial}{\partial x_j} \left(\frac{\partial v_i}{\partial x_j} \right) \quad (7)$$

Energy conservation equation for fluid domain:

$$\rho C_p \frac{\partial(T)}{\partial t} + \rho C_p \frac{\partial(v_j T)}{\partial x_j} = k_f \frac{\partial}{\partial x_j} \left(\frac{\partial T}{\partial x_j} \right) \quad (8)$$

Energy conservation equation for solid domain:

$$\frac{\partial}{\partial x_j} \left(\frac{\partial T}{\partial x_j} \right) = \frac{1}{\alpha} \frac{\partial T}{\partial t} \quad (9)$$

Here v_i represents the velocity components in i^{th} directions. P , t , and T represent the pressure, time, and temperature, respectively. The c_p and α represent the fluid-specific heat and thermal diffusivity of heat sink material.

3.2 Computational Details

In ANSYS/FLUENT software, the discretization of the governing equation is obtained by the finite volume method. The second-order upwind scheme is used for spatial discretization of the energy and momentum equation. The pressure velocity coupling is obtained by using the SIMPLE algorithm. The scale residuals of equations are employed at 10^{-6} .

While the heat sink is moving, the mesh of the fluid near the heat sink must be regenerated. Thus, the layering technique has been employed in the dynamic mesh setup. In order to ensure the results of the numerical study are independent of the occupied number of cells and the considered time step, a mesh independency, and time independency test are established. Figure 3 (a) shows the eight levels of grids, such as 234 556, 324 568, 435 892, 498 460, 522 764, 580 356, 784 322, 985 662, are tested. The percentage difference of time-averaged Nusselt number with the number of cells of 522 764 compared to 580 356 cells is less than 1%. As shown in Figure 3 (b), three-time steps are considered ($\tau/8$, $\tau/16$, and $\tau/32$). The percentage difference of peak-to-peak area-averaged Nusselt number with a time step of $\tau/16$ compared to $\tau/32$ is within 1%. Therefore, the mesh with the number of cells of 522,764 and a time step of $\tau/16$ is selected as the optimum mesh and time step on which all results are presented.

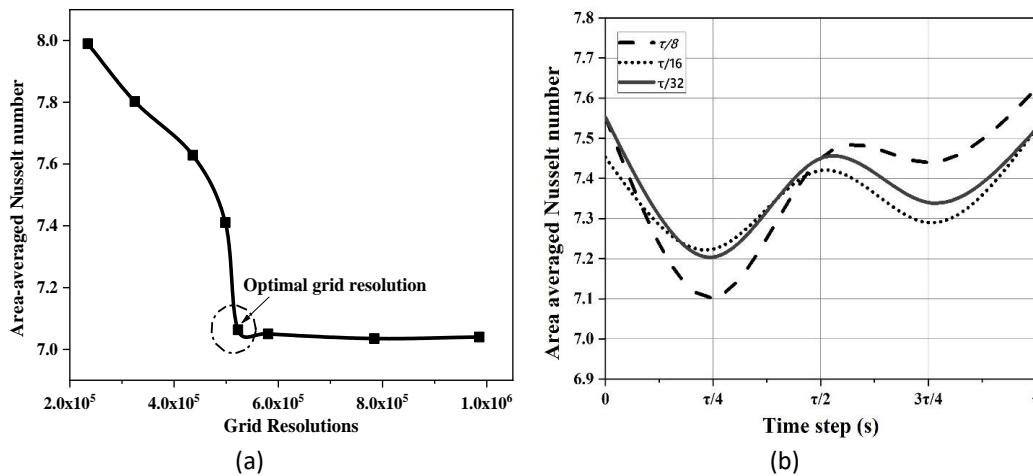


Fig. 3. (a) Variation of area-averaged Nusselt number with different mesh levels (b) with different time steps

As shown in Figure 4, the present numerical findings are validated with experimental results under sinusoidal vibration with a Reynolds number of 520 and supplied heat of 2666 W/m^2 . As mentioned by Siriwardana *et al.*, [39], this supplied heat follows the generated heat load of tape storage data servers. It is to be noted that the experiment was performed under low supplied heat and Reynolds number conditions due to limited resources; hence, the experiment is used merely for validation. However, as noted in the studies of [40,41], the current study conducted the numerical investigation under actual supplied heat and Reynolds number conditions of data servers. As seen in Figure 4, the experimental results are close to CFD modelling, with a maximum variation of 2.4%

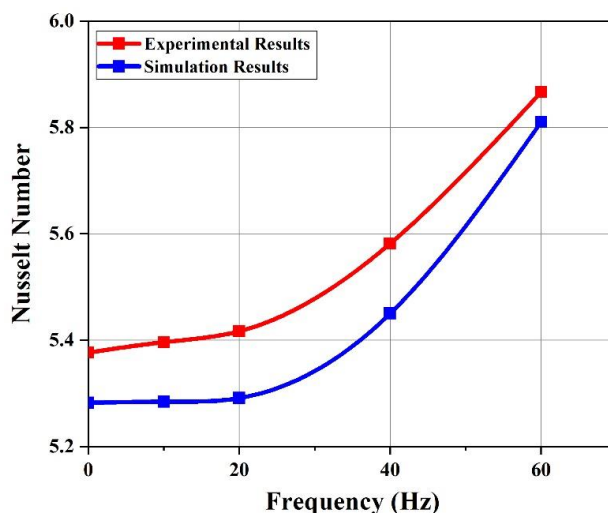


Fig. 4. Nusselt number validation with experimental results

4. Results and Discussion

Initially, the numerical analysis was performed under non-vibrating conditions at $Re = 1000$. Then, the comparative analysis of heat transfer enhancement of the vertically and horizontally vibrating heat sink was performed under the range of vibrational frequency and peak-to-peak amplitude of 0-80 Hz and 0- 0.005 m, respectively. The vibrating directions are mentioned in Figure 5 using black arrows in the cross-section view of the heat sink.

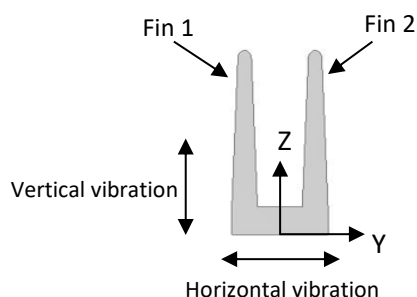


Fig. 5. Cross-section of the heat sink

Thermal boundary layer development on the heat sink surfaces is expected to disrupt by the influence of vertical and horizontal vibration under sinusoidal and square wave shapes of the heat sink by setting the fluid in motion. Therefore, a comparison of velocity vectors under non-vibration, vertical and horizontal vibration at each vibration wave shape at different stages of cycle time is needed. Thus, velocity profiles of no-vibration conditions induced by vertical and horizontal vibration at each cycle time are discussed below.

Figure 6 shows the planar representation of transient velocity vectors going through a cross-section of the heat sink at non-vibrating and vertically vibrating conditions at the frequency and peak-to-peak amplitude of 80 Hz and 0.003 m. As shown in Figure 6 (a), when the heat sink is at static condition, flow streamlines move from inlet to outlet without any perturbation. When the heat sink begins the first quartile of the sinusoidal vibration (Figure 6 (b)), the heat sink starts to move upward and flow within the channel area moved upwards and circulate over the lateral surfaces of both fins.

When the heat sink moved upward further to the beginning of the second quarter of the sinusoidal motion (Figure 6 (c)), perturbations within the flow regime were found to be very small. At the beginning of the third quarter of the sinusoidal motion (Figure 6 (d)), the heat sink moved downward, and fluid outside the fins started to circulate over the lateral surfaces of both fins. Moreover, flow within the channel area moved downward, hitting the base of the channel area. When the heat sinks further moved downward toward the beginning of the fourth quarter (Figure 6 (e)), the flow profile is similar to Figure 6 (b)).

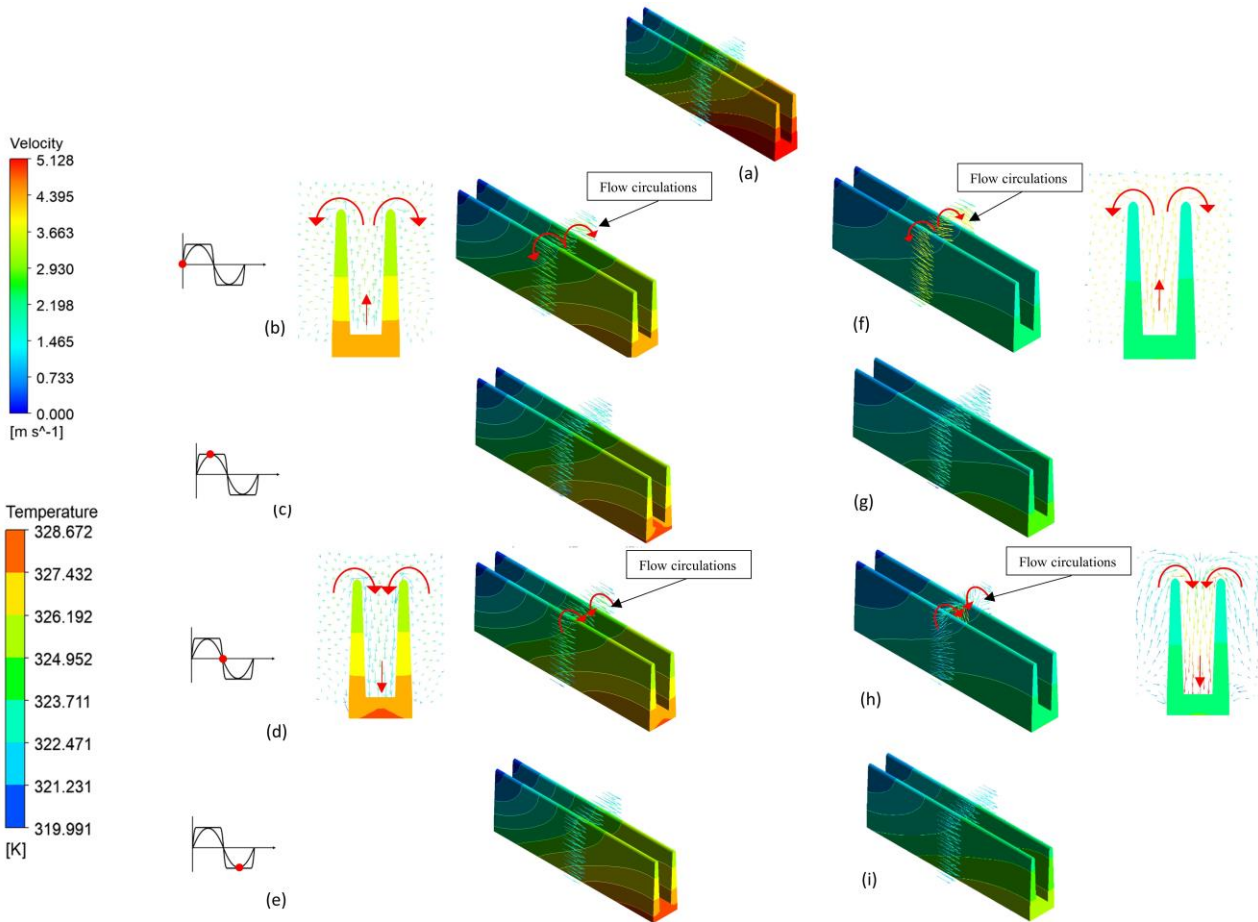


Fig. 6. Planar representation of transient velocity vectors going through the cross-section of the vertically vibrating heat sink at various cycle stages at the frequency (80 Hz), peak to peak amplitude (0.003m), and Reynolds number (1000) (a) static (b) sinusoidal at 1st quartile of the cycle (c) sinusoidal at 2nd quartile of the cycle (d) sinusoidal at 3rd quartile of the cycle (e) sinusoidal at 4th quartile of the cycle (f) square at 1st quartile of the cycle (g) square at 2nd quartile of the cycle (h) square at 3rd quartile of the cycle (i) square at 4th quartile of the cycle

When the square wave-shaped vibration is utilized, the heat sink suddenly starts to move upward to its maximum positive amplitude. Thus, at the beginning of the first quarter of the vibration, flow within the channel area moved upwards, and strong flow circulation occurred at the tip of both fins, as shown in Figure 6 (f). However, after reaching its maximum positive amplitude, the heat sink remains at maximum deflection till the end of the first vibration quartile. Thus, the flow profile remained similar to no-vibration conditions at the start of the second vibration quartile, as shown in Figure 6 (g). However, at the beginning of the third vibration quartile, the heat sinks instantly moved downward, which induced strong flow recirculation over the tip of the fins and hit the base of the

channel area, as shown in Figure 6 (h). Finally, when the heat sink is at the beginning of the fourth quarter of the vibration (Figure 6 (i)), the flow profile is similar to Figure 6 (g).

Figure 7 shows the planar representation of transient velocity vectors going through the cross-section of the heat sink at horizontal vibration at the frequency and peak-to-peak amplitude of 80 Hz and 0.003 m. When the heat sink is at the beginning of the first quarter of the horizontal sinusoidal vibration (Figure 7 (a)), the heat sink starts to move right side, and it induces the counterclockwise airflow circulations over both fins and hits the outer surface of the fin 1. Moreover, the flow within the channel area follows the displacement direction and hits the surface of fin 2. When the heat sink moved to the right side further to the beginning of the second quarter of the sinusoidal motion (Figure 7(b)), airflow circulations shed into two counterclockwise recirculation zones near the tip of the fins. At the beginning of the third quarter of the sinusoidal motion, the heat sink moved left side, and fluid outside the heat sink started to recirculate over both fins and hit the outer surface of fin 2, as shown in Figure 7 (c). Moreover, flow within the channel area moved left side, hitting the surface of fin1. When the heat sinks further moved left side toward the beginning of the fourth quarter (Figure 7 (d)), the flow profile is opposite to Figure 7 (b)).

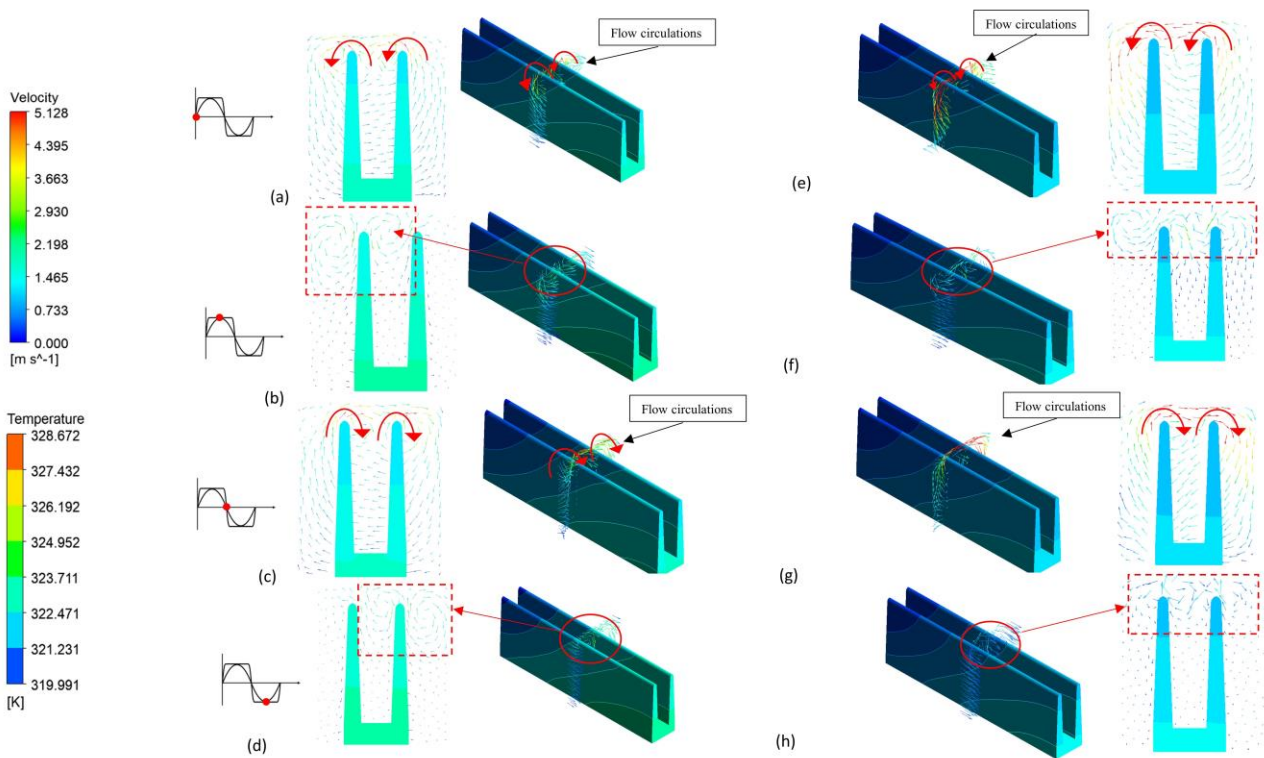


Fig. 7. Planar representation of transient velocity vectors going through the cross-section of the horizontally vibrating heat sink at various cycle stages at the frequency (80 Hz), peak to peak amplitude (0.003m), and Reynolds number (1000) (a) static (b) sinusoidal at 1st quartile of the cycle (c) sinusoidal at 2nd quartile of the cycle (d) sinusoidal at 3rd quartile of the cycle (e) sinusoidal at 4th quartile of the cycle (f) square at 1st quartile of the cycle (g) square at 2nd quartile of the cycle (h) square at 3rd quartile of the cycle (i) square at 4th quartile of the cycle

At the start of the first quartile of square wave-shaped horizontal vibration (Figure 7(e)), the heat sink suddenly starts to move to the right side to its maximum positive amplitude. It induces strong airflow circulations around both fins compared to the sinusoidal vibration and circulated flow hitting the outer surface of fin 1. Also, the flow within the channel area follows the movement direction of the heat sink and hits the surface of fin 2. At the start of the second quartile, the heat sink remains

at maximum deflection until the end of the first quarter. Thus, strong airflow recirculation gradually diminishes into perturbations around the tips of both fins, as shown in Figure 7(f). At the start of the third quartile (Figure 7(g)), the heat sinks instantly started to move to its maximum negative amplitude, which led to a strong airflow circulation over the tip of the fins and hitting the outer surface of fin 2. Moreover, fluid within the channel area hits the surface of fin 1. When the heat sink is at the start of the fourth quartile (Figure 6 (h)), the flow profile is found to be similar to Figure 6 (f).

As shown in Figure 6 and Figure 7, vertical and horizontal vibrations induce the recirculation zones within the flow field. However, the horizontal vibration of the heat sink under both wave shapes creates strong flow recirculation over the fins compared to vertical vibration, resulting in an intensive mixing effect. Moreover, horizontal vibration induces secondary flows, which hit the large area of lateral surfaces of fins, while vertical vibration leads to the mixing of air particles, which only hits the base of the channel area of the heat sink. Thus, horizontal vibration induces more disturbance on the thermal boundary layer near the heated surfaces of fins than vertical vibration, leading to higher thermal performance. Furthermore, as shown in the velocity profiles, strong recirculation zones are induced with square wave-shaped vibration compared to the sinusoidal wave shape at each vibrational direction owing to impulsive motion, resulting in higher disturbance to the thermal boundary layer, thereby enhancing the heat transfer further.

Figure 8 shows the effect of vibration on temperature contours on the planes passing through the cross-section and tip of the heat sink under no vibration and different vibration conditions. It is seen in Figure 6 (a) the fluid flow is streamlined under non-vibrating conditions. Thus, the thermal boundary layer of the non-vibrating heat sink has a high-temperature gradient near the heat sink surfaces, thereby restricting the heat transfer, as observed in Figure 8 (a).

However, when the heat is subjected to vibration, the continuous formation of flow recirculation disrupts the thermal boundary layer and enhances heat transfer. Figure 8 (b-c) shows the effect of vertical vibrational frequency on the thermal boundary layer. Applying vertical vibration leads to a low-temperature region near the fins, and thermal wakes behind the fins lead to spread, leading to higher heat transfer in both fins. When square wave-shaped vibration is used (Figure 8 (c)), the thickness of the thermal boundary layer is reduced, and the disturbance to the thermal wake behind the fins is widely spread, thereby disseminating higher heat from the heat sink to the air, thus a higher cooling effect. As shown in Figure 8 (d-e), when the vibrational peak-to-peak amplitude increases, the air temperature around the fins decreases further, thereby decreasing the temperature of the fins. However, the air temperature surrounding the fins is lower with square wave-shaped vibration, thus having a higher cooling effect on the fins.

When the horizontal vibration is applied, the airflow recirculates and hits the heated fins. Thus, As shown in Figure 8 (f-g), the heat started to widely disseminate over the fluid domain, leading to an air temperature decrease adjacent to the fin surfaces, resulting in a higher cooling effect. However, increased frequency under square wave-shaped vibration further decreases air temperature near the fin surfaces due to stronger secondary flows, leading to a higher cooling effect, as seen in Figure 8 (g). Figure 8 (h-i) shows the effect of increasing horizontal vibration amplitude on the thermal boundary layer under both wave shapes. It can be observed that with increasing peak-to-peak amplitude from 0.003 m to 0.005 m, air temperature adjacent to the fins further decreases due to the strong flow disturbances induced by higher amplitude and application of square wave-shaped vibration shows the lowest air temperature profile near the fins, resulting higher heat transfer of the fins.

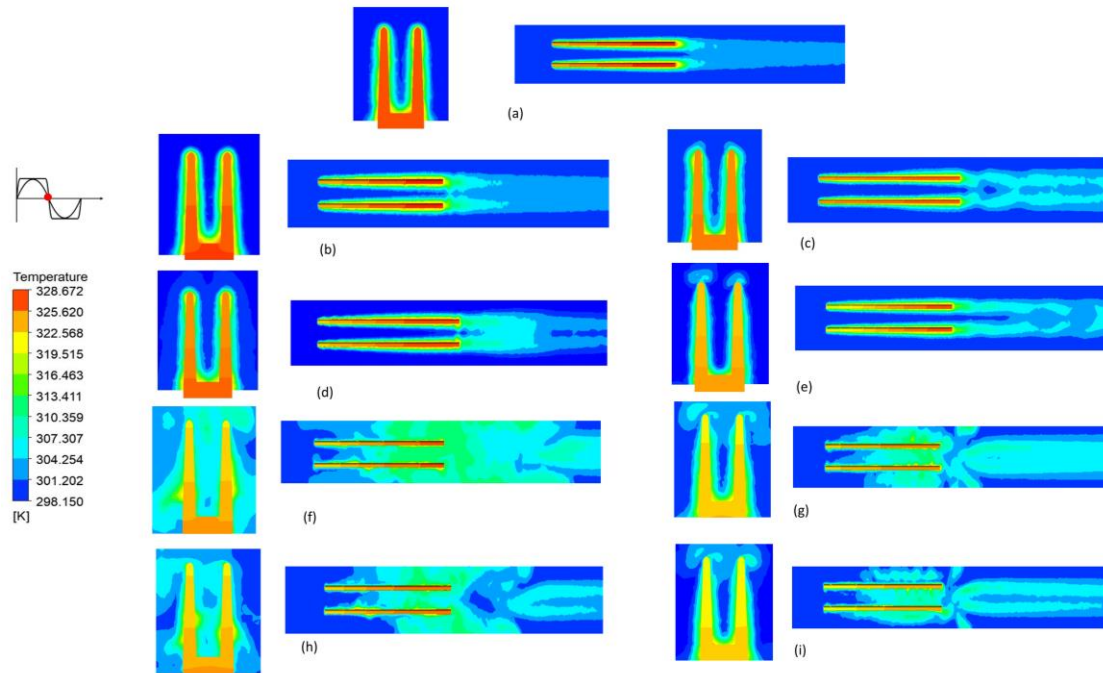


Fig. 8. Planar representation of temperature contours going through the cross-section and tip of the heat sink at various vibrating conditions (a) static (b) vertical sinusoidal oscillation at $f = 80$ Hz, Amp = 0.003 m (c) vertical square oscillation $f = 80$ Hz, Amp = 0.003 m (d) vertical sinusoidal oscillation at $f = 80$ Hz, Amp = 0.005 m (e) vertical square oscillation $f = 80$ Hz, Amp = 0.003 m (f) horizontal sinusoidal oscillation at $f = 80$ Hz, Amp = 0.003 m (g) horizontal square oscillation $f = 80$ Hz, Amp = 0.003 m (h) horizontal sinusoidal oscillation at $f = 80$ Hz, Amp = 0.005 m (i) horizontal square oscillation $f = 80$ Hz, Amp = 0.003 m

Figure 9 shows the variation of time-averaged Nusselt numbers with vibrational characteristics under sinusoidal and square wave-shaped vibration. The current study obtains Nusselt numbers of the vertically vibrating heat sink, while the Nusselt numbers of the horizontally vibrating heat sink are obtained by the previous study performed by Rasangika *et al.*, [37]. As shown in Figure 9 (a), enhancement of the Nusselt number with vertical vibration is found to be insignificant up to 40 Hz frequency. This is because the vibrational frequencies below 40 Hz are insufficient to induce flow perturbation to disrupt the thermal boundary layer. However, Rasangika *et al.*, [37] found that the enhancement of the Nusselt number is insignificant up to 30 Hz with horizontal vibration. This lower threshold frequency could be attributed to the higher mixing effect of the flow induced by the horizontal vibration compared to the vertical vibration. When the applied frequency of vertical vibration is higher than this threshold frequency (40 Hz), the Nusselt number exponentially increases with an increase in frequency. Moreover, the utilization of vibration with square wave shape provides a greater enhancement in Nusselt number compared to the sinusoidal vibration at every frequency level. The impulsive up-and-down motion of the heat sink under square wave-shaped vibration induces strong flow circulations around the lateral surfaces of the heat sink, resulting in higher heat transfer. Based on the study of the Rasangika *et al.*, [37], the higher enhancement in Nusselt value can be achieved by applying the horizontal vibration in comparison with vertical vibration at every frequency level under both wave shapes. It is noteworthy to mention that a higher Nusselt number value could be achieved with horizontal sinusoidal motion compared to vertical square wave-shaped vibration at similar frequency values. Compared to the non-vibrating heat sink, the Nusselt number is increased up to 7.1% and 6% with vertical vibration at the vibrational frequency and amplitude of 80 Hz and 0.003 m with square and sinusoidal vibration, respectively. However,

Rasangika *et al.*, [37] obtained Nusselt number enhancement up to 13.7% and 8.2% with horizontal vibration at similar vibration conditions with square and sinusoidal vibrations, respectively.

Figure 9 (b) represents the Nusselt number variation with respect to peak-peak amplitude. A rise in peak-to-peak amplitude leads to an enhancement in the Nusselt number for both sinusoidal and square wave shapes. Increased vibration amplitude induces strong flow circulation around the heat sink, resulting in a higher heat transfer rate. However, the enhancement is dominant with square wave-shaped vibration at each vibrational amplitude condition. This can be attributed to the stronger flow circulations caused by the square wave-shaped vibration due to its sudden upward and downward motion. However, Rasangika *et al.*, [37] recorded a greater enhancement in the Nusselt number by utilizing the horizontal vibration at each peak-to-peak amplitude level under both wave shapes. Utilization of vertical vibration with square and sinusoidal vibration at $f = 80$ Hz and Amp = 0.005 m leads to an 8.6 % and 7.2% enhancement in Nusselt numbers, while enhancement with horizontal vibration is recorded as 15.3% and 10.4%, respectively.

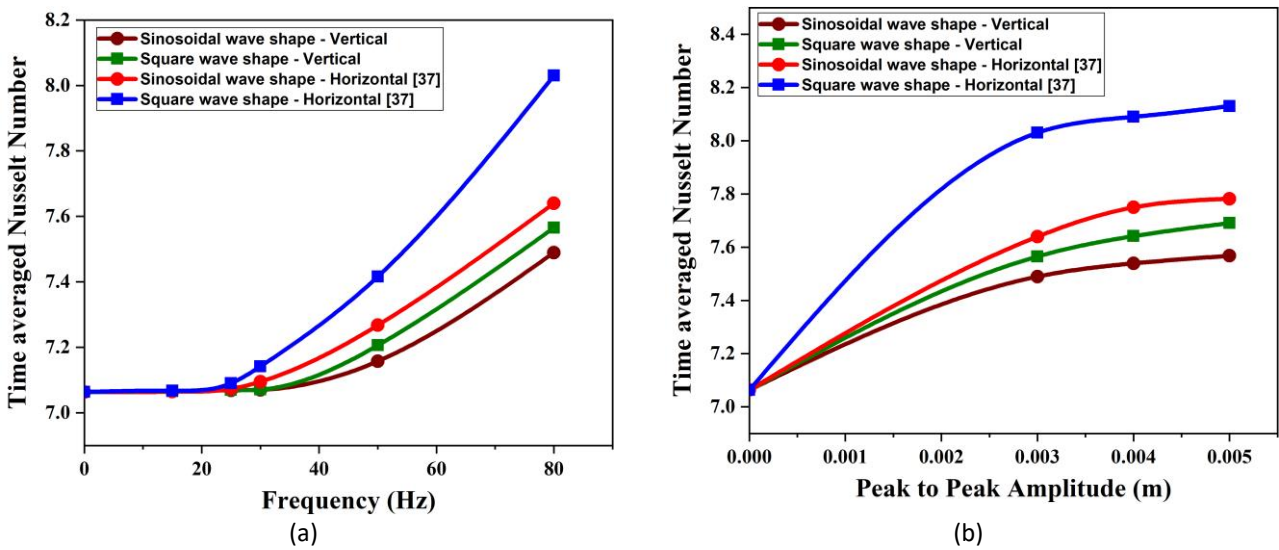


Fig. 9. Time averaged Nusselt number variation at $Re = 1000$ (a) vibrational frequency at the peak-to-peak amplitude of 0.003 m (b) vibrational peak-peak amplitude at frequency of 80 Hz

$$\text{Nusselt ratio} = \frac{\text{Nusselt number with vibration}}{\text{Nusselt number without vibration}} \quad (10)$$

As shown in Figure 9, an increase in vibration characteristics leads to enhancement in the Nusselt number under both wave shapes, while horizontal vibration shows a prominent effect on the enhancement of the Nusselt number. In order to perform a comparative analysis and estimate the enhancement of the Nusselt number under both vibrational directions, the Nusselt ratio is calculated using Eq. (10). Figure 10 shows the variation of the Nusselt ratio with vibrational frequency and peak-to-peak amplitude obtained by the study of Rasangika *et al.*, [37] and the current study. As shown in Figure 10 (a), an increase in frequency leads to an increase in the Nusselt ratio, while square wave-shaped vibration provides a greater enhancement in the Nusselt ratio at every frequency value. However, Rasangika *et al.*, [37] obtained higher Nusselt ratios with a lower threshold frequency value than vertical vibration under both wave shapes at each vibrational frequency. In comparison with non-vibrating conditions, vertical vibration showed a maximum Nusselt ratio enhancement of 7.1% and 6% with square and sinusoidal wave shapes, respectively. On the other hand, Rasangika *et al.*, [37] obtained 13.7 % and 8.2 % enhancement of the Nusselt ratio with square and sinusoidal wave shapes under similar vibration frequencies. Furthermore, it is interesting to note that the similar

thermal performance of a vertically vibrating heat sink could be obtained by applying horizontal vibration at a lower frequency level. For instance, the Nusselt ratio (1.071) obtained with vertical vibration at 80 Hz could be achieved with horizontal vibration at a frequency of approximately 58 Hz. These results revealed that the application of horizontal vibration on the cooling system is more efficient and economical than vertical vibration.

As shown in Figure 10 (b), the Nusselt ratio increases with increasing peak-peak amplitude of vertical vibration, and the relative enhancement of the Nusselt ratio is dominant with square wave-shaped vibration. However, Rasangika *et al.*, [37] obtained higher Nusselt ratio values than vertical vibration at each vibrational peak-to-peak amplitude under both wave shapes. As compared to the non-vibrating heat sink, vertical vibration showed maximum Nusselt ratio enhancement of 8.6 % and 7.2 % with square and sinusoidal wave shapes, respectively. However, Rasangika *et al.*, [37] obtained a 15.3% and 10.4% enhancement of the Nusselt ratio with square and sinusoidal wave shapes under similar vibration peak-to-peak amplitudes. As discussed above, a similar Nusselt ratio of a vertically vibrating heat sink could be achieved by utilizing horizontal vibration at a lower amplitude level. As highlighted in Figure 10 (b), the Nusselt ratio (1.086) obtained with vertical vibration at the peak-to-peak amplitude of 0.005m could be achieved with horizontal vibration at the peak-to-peak amplitude of approximately 0.0015 m.

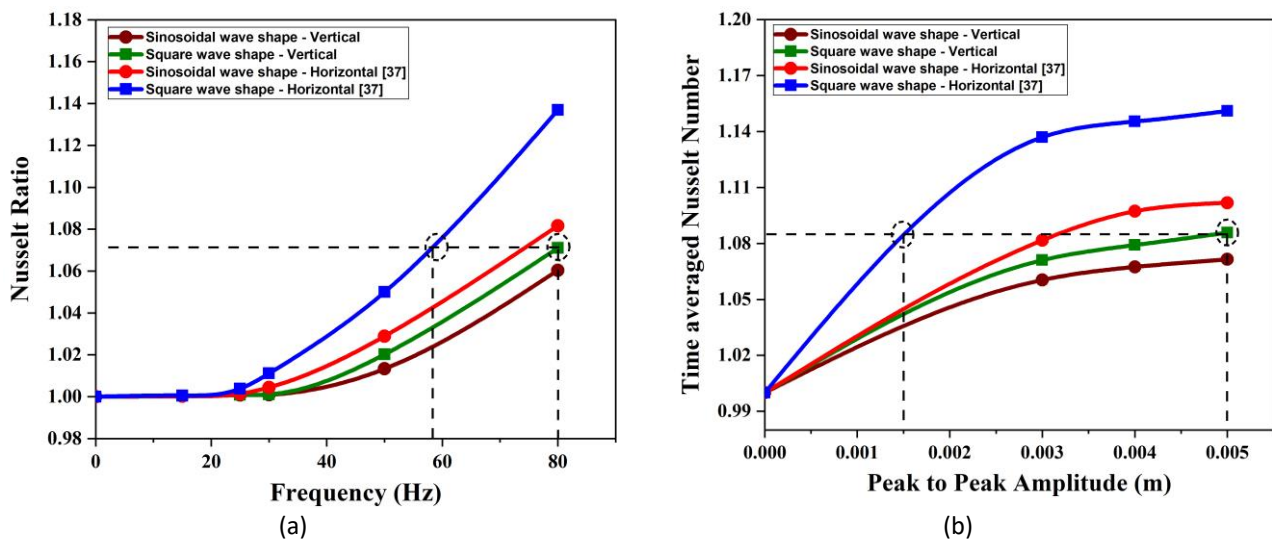


Fig. 10. Variation of Nusselt ratio at $Re = 1000$ (a) vibrational frequency at the peak-peak amplitude of 0.003m (b) vibrational peak-peak amplitude at frequency of 80 Hz

5. Conclusion

The thermal efficiency of vertically vibrating conventional heat sink has been investigated under sinusoidal and square wave shapes. The study has been performed for vibrational frequency and amplitude range of 0-80 Hz and 0-0.005 m, respectively. The numerical results are validated against experimental results with a 2.4 % deviation. It was found that the application of vertical vibration improves the Nusselt number at higher vibrational frequencies ($f > 40$ Hz) and amplitudes by inducing the flow circulations adjacent to the heat sink. Due to the impulsive up-and-down motion of the heat sink under square wave-shaped vibration, a higher enhancement in the Nusselt value is obtained as compared to the sinusoidal vibration at every level of vibrational characteristics. A maximum of 8.6% enhancement in Nusselt number was obtained with square wave-shaped vibration, while 7.2% enhancement was recorded with sinusoidal vibrations at $f = 80$ Hz and amplitude of 0.005m. Therefore, the application of vibration in the electronic cooling system is beneficial to the

enhancement of heat transfer, and this enhanced cooling effect can be utilized to miniaturize the electronic cooling system. Moreover, the result of the current study is compared with the previous study, and it was concluded that the heat transfer enhancing effect of vibration is dominant with horizontal vibration compared to vertical vibration. Therefore, the application of horizontal vibration leads to a similar thermal performance of the vertical vibrating cooling system under lower vibration conditions and thereby saving the cost of the cooling system as compared to the vertical vibration. Regardless of promising features, this mechanism may cause device reliability and stability issues in the cooling system due to the formation of fatigue stress on the vibrating surface. Thus, special consideration is required to evaluate the reliability of the vibrating cooling system.

Acknowledgment

The authors would like to thank the Ministry of Higher Education (MOHE), Malaysia for providing financial assistance under the Fundamental Research grant Scheme (FRGS/1/2018/TK03/UTP/02/7) and Universiti Teknologi PETRONAS for providing the required facilities to conduct this research work.

References

- [1] Dizaji, Hamed Sadighi, Eric Hu, Lei Chen, Samira Pourhedayat, and Makatar Wae-hayee. "Proposing the concept of mini Maisotsenko cycle cooler for electronic cooling purposes; experimental study." *Case Studies in Thermal Engineering* 27 (2021): 101325. <https://doi.org/10.1016/j.csite.2021.101325>
- [2] Bhandari, Prabhakar, and Yogesh K. Prajapati. "Thermal performance of open microchannel heat sink with variable pin fin height." *International journal of thermal sciences* 159 (2021): 106609. <https://doi.org/10.1016/j.ijthermalsci.2020.106609>
- [3] Hua, Weisan, Liyu Zhang, and Xuelai Zhang. "Research on passive cooling of electronic chips based on PCM: A review." *Journal of Molecular Liquids* 340 (2021): 117183. <https://doi.org/10.1016/j.molliq.2021.117183>
- [4] Japar, Wan Mohd Arif Aziz, Nor Azwadi Che Sidik, Natrah Kamaruzaman, Yutaka Asako, and Nura Mu'az Muhammad. "Hydrothermal performance in the Hydrodynamic Entrance Region of Rectangular Microchannel Heat Sink." *Journal of Advanced Research in Numerical Heat Transfer* 1, no. 1 (2020): 22-31.
- [5] Bouhafis, Mohammed, Abed Meghdir, Abdelaziz Adjeloua, and Houari Ameer. "Numerical Simulation of the Fin Impact on the Cooling of the Shell of a Rotary Kiln." *Journal of Advanced Research in Fluid Mechanics and Thermal Sciences* 103, no. 2 (2023): 68-84. <https://doi.org/10.37934/arfmts.103.2.6884>
- [6] Wang, Bo-Fu, Quan Zhou, and Chao Sun. "Vibration-induced boundary-layer destabilization achieves massive heat-transport enhancement." *Science advances* 6, no. 21 (2020): eaaz8239. <https://doi.org/10.1126/sciadv.aaz8239>
- [7] Yu, Xiaoyong, Yonghao Zhang, Songwei Li, Luguo Liu, Yazhe Lu, Shouxu Qiao, and Sichao Tan. "Simultaneous measurement of the structures of the velocity and thermal boundary layers in the rod bundle channel." *International Journal of Heat and Mass Transfer* 192 (2022): 122906. <https://doi.org/10.1016/j.ijheatmasstransfer.2022.122906>
- [8] Kannan, K. Gopi, and R. Kamatchi. "Experimental investigation on thermosyphon aid phase change material heat exchanger for electronic cooling applications." *Journal of Energy Storage* 39 (2021): 102649. <https://doi.org/10.1016/j.est.2021.102649>
- [9] Tsai, Wei-Yu, Guan-Rong Huang, Kuang-Kuo Wang, Chin-Fu Chen, and J. C. Huang. "High thermal dissipation of Al heat sink when inserting ceramic powders by ultrasonic mechanical coating and armoring." *Materials* 10, no. 5 (2017): 454. <https://doi.org/10.3390/ma10050454>
- [10] Cai, Jun, Xunfeng Li, Bin Liu, and Xiulan Huai. "Effect of cavitating flow on forced convective heat transfer: a modeling study." *Chinese science bulletin* 59 (2014): 1580-1590. <https://doi.org/10.1007/s11434-014-0205-x>
- [11] Liu, Bin, Jun Cai, Xiulan Huai, and Fengchao Li. "Cavitation bubble collapse near a heated wall and its effect on the heat transfer." *Journal of heat transfer* 136, no. 2 (2014). <https://doi.org/10.1115/1.4024071>
- [12] Hoi, Su Min, An Liang Teh, Ean Hin Ooi, Irene Mei Leng Chew, and Ji Jinn Foo. "Plate-fin heat sink forced convective heat transfer augmentation with a fractal insert." *International Journal of Thermal Sciences* 142 (2019): 392-406. <https://doi.org/10.1016/j.ijthermalsci.2019.04.035>
- [13] Léal, L., Marc Miscevic, Pascal Lavieille, M. Amokrane, François Pigache, Frédéric Topin, Bertrand Nogarède, and L. Tadrist. "An overview of heat transfer enhancement methods and new perspectives: Focus on active methods using electroactive materials." *International Journal of heat and mass transfer* 61 (2013): 505-524. <https://doi.org/10.1016/j.ijheatmasstransfer.2013.01.083>

- [14] Zhang, Qingyuan, Zhenfei Feng, Zhenzhou Li, Zhen Chen, Shizhao Huang, Jinxin Zhang, and Fangwen Guo. "Numerical investigation on hydraulic and thermal performances of a mini-channel heat sink with twisted ribs." *International Journal of Thermal Sciences* 179 (2022): 107718. <https://doi.org/10.1016/j.ijthermalsci.2022.107718>
- [15] Ranjbar, Ali Mohammad, Zeinab Pouransari, and Majid Siavashi. "Improved design of heat sink including porous pin fins with different arrangements: A numerical turbulent flow and heat transfer study." *Applied Thermal Engineering* 198 (2021): 117519. <https://doi.org/10.1016/j.applthermaleng.2021.117519>
- [16] Elfaghi, Abdulhafid MA, Alhadi A. Abosbaia, Munir FA Alkbir, and Abdoulhdi AB Omran. "Heat Transfer Enhancement in Pipe Using Al₂O₃/Water Nanofluid." *CFD Letters* 14, no. 9 (2022): 118-124. <https://doi.org/10.37934/cfdl.14.9.118124>
- [17] Hassan, Qais Hussein, Shaalan Ghanam Afluq, and Mohamed Abed Al Abas Siba. "Numerical investigation of heat transfer in car radiation system using improved coolant." *Journal of Advanced Research in Fluid Mechanics and Thermal Sciences* 83, no. 1 (2021): 61-69. <https://doi.org/10.37934/arfmts.83.1.6169>
- [18] Urmi, Wajiha Tasnim, A. S. Shafiqah, Md Mustafizur Rahman, Kumaran Kadirgama, and Md Abdul Maleque. "Preparation methods and challenges of hybrid nanofluids: a review." *Journal of Advanced Research in Fluid Mechanics and Thermal Sciences* 78, no. 2 (2020): 56-66. <https://doi.org/10.37934/arfmts.78.2.5666>
- [19] Safiei, Wahaizad, Md Mustafizur Rahman, Ratnakar Kulkarni, Md Noor Ariffin, and Zetty Akhtar Abd Malek. "Thermal conductivity and dynamic viscosity of nanofluids: a review." *Journal of Advanced Research in Fluid Mechanics and Thermal Sciences* 74, no. 2 (2020): 66-84. <https://doi.org/10.37934/arfmts.74.2.6684>
- [20] Mohammadi, Majid, Amin Taheri, Mohammad Passandideh-Fard, and Mohammad Sardarabadi. "Electronic chipset thermal management using a nanofluid-based mini-channel heat sink: An experimental study." *International Communications in Heat and Mass Transfer* 118 (2020): 104836. <https://doi.org/10.1016/j.icheatmasstransfer.2020.104836>
- [21] Moghanlou, Farhad Sadegh, Amin Shams Khorrami, Esmail Esmailzadeh, and Habib Aminfar. "Experimental study on electrohydrodynamically induced heat transfer enhancement in a minichannel." *Experimental Thermal and Fluid Science* 59 (2014): 24-31. <https://doi.org/10.1016/j.expthermflusci.2014.07.019>
- [22] Testi, Daniele, Francesco D'Ettorre, Davide Della Vista, and Walter Grassi. "Parabolic flight results of electrohydrodynamic heat transfer enhancement in a square duct." *International Journal of Thermal Sciences* 117 (2017): 1-13. <https://doi.org/10.1016/j.ijthermalsci.2017.03.015>
- [23] Thakar, Shridhar S., Sannil Nambiar, Gaurav A. Chandavarkar, and S. Senthur Prabu. "Investigation of impingement cooling on a heat sink using CFD simulation." *Materials Today: Proceedings* 46 (2021): 8753-8760. <https://doi.org/10.1016/j.matpr.2021.04.066>
- [24] Gil, Paweł. "Experimental investigation on heat transfer enhancement of air-cooled heat sink using multiple synthetic jets." *International Journal of Thermal Sciences* 166 (2021): 106949. <https://doi.org/10.1016/j.ijthermalsci.2021.106949>
- [25] Jiang, Li-Jia, Shou-Li Jiang, Wen-Long Cheng, Yong-Le Nian, and Rui Zhao. "Experimental study on heat transfer performance of a novel compact spray cooling module." *Applied Thermal Engineering* 154 (2019): 150-156. <https://doi.org/10.1016/j.applthermaleng.2019.03.078>
- [26] Shalaby, M. A., El-Negiry El-Negiry, Emad Abd El-Laitef, and H. El-Tahan. "Forced Convection Heat Transfer from Oscillating Horizontal Cylinder." *MEJ. Mansoura Engineering Journal* 28, no. 4 (2021): 1-14. <https://doi.org/10.21608/bfemu.2021.142396>
- [27] Pottebaum, Tait Sherman, and Mory Gharib. "Using oscillations to enhance heat transfer for a circular cylinder." *International Journal of Heat and Mass Transfer* 49, no. 17-18 (2006): 3190-3210. <https://doi.org/10.1016/j.ijheatmasstransfer.2006.01.037>
- [28] Sreenivasan, K., and A. Ramachandran. "Effect of vibration on heat transfer from a horizontal cylinder to a normal air stream." *International Journal of Heat and Mass Transfer* 3, no. 1 (1961): 60-67. [https://doi.org/10.1016/0017-9310\(61\)90006-0](https://doi.org/10.1016/0017-9310(61)90006-0)
- [29] Gau, C., J. M. Wu, and C. Y. Liang. "Heat transfer enhancement and vortex flow structure over a heated cylinder oscillating in the crossflow direction." (1999): 789-795. <https://doi.org/10.1115/1.2826067>
- [30] Dawood, A. S., B. L. Manocha, and S. M. J. Ali. "The effect of vertical vibrations on natural convection heat transfer from a horizontal cylinder." *International Journal of Heat and Mass Transfer* 24, no. 3 (1981): 491-496. [https://doi.org/10.1016/0017-9310\(81\)90056-9](https://doi.org/10.1016/0017-9310(81)90056-9)
- [31] Karanth, D., G. W. Rankin, and K. Sridhar. "A finite difference calculation of forced convective heat transfer from an oscillating cylinder." *International journal of heat and mass transfer* 37, no. 11 (1994): 1619-1630. [https://doi.org/10.1016/0017-9310\(94\)90177-5](https://doi.org/10.1016/0017-9310(94)90177-5)

- [32] Shokouhmand, H., and SMA Noori Rahim Abadi. "Finite element analysis of natural heat transfer from an isothermal array of cylinders in presence of vertical oscillations." *Heat and mass transfer* 46 (2010): 891-902. <https://doi.org/10.1007/s00231-010-0645-z>
- [33] Shokouhmand, H., S. M. A. Noori Rahim Abadi, and A. Jafari. "The effect of the horizontal vibrations on natural heat transfer from an isothermal array of cylinders." *International Journal of Mechanics and Materials in Design* 7 (2011): 313-326. <https://doi.org/10.1007/s10999-011-9170-6>
- [34] Gururatana, Suabsakul, and Xianchang Li. "Heat transfer enhancement of small scale heat sinks using vibrating pin fin." *Am. J. Sci* 10 (2013): 801-809. <https://doi.org/10.3844/ajassp.2013.801.809>
- [35] Rahman, Aevelina, and Danesh Tafti. "Characterization of heat transfer enhancement for an oscillating flat plate-fin." *International Journal of Heat and Mass Transfer* 147 (2020): 119001. <https://doi.org/10.1016/j.ijheatmasstransfer.2019.119001>
- [36] Najim, Riyah, Wahib, Jamal Hami, Jalil, Saad Mohammed and Ibrahim Fat'hi, Mohammed. "Experimental Study of the Effect of Vertical Oscillation on Forced Convection Coefficient from Vertical Channel", *Anbar Journal Engineering Sciences* (2013) 260.
- [37] Rasangika, Ambagaha Hewage Dona Kalpani, Mohammad Shakir Nasif, William Pao, and Rafat Al-Waked. "Numerical Investigation of the Effect of Square and Sinusoidal Waves Vibration Parameters on Heat Sink Forced Convective Heat Transfer Enhancement." *Applied Sciences* 12, no. 10 (2022): 4911. <https://doi.org/10.3390/app12104911>
- [38] Kalpani Rasangika, Ambgaha Hewage Dona, Mohammad Shakir Nasif, William Pao, and Rafat Al-Waked. "Numerical Investigation on the Effect of Vibration on Cooling Enhancement of Heat Sinks." In *ICPER 2020: Proceedings of the 7th International Conference on Production, Energy and Reliability*, pp. 171-178. Singapore: Springer Nature Singapore, 2022. https://doi.org/10.1007/978-981-19-1939-8_15
- [39] Siriwardana, Jayantha, Saliya Jayasekara, and Saman K. Halgamuge. "Potential of air-side economizers for data center cooling: A case study for key Australian cities." *Applied Energy* 104 (2013): 207-219. <https://doi.org/10.1016/j.apenergy.2012.10.046>
- [40] Ebrahimi, Khosrow, Gerard F. Jones, and Amy S. Fleischer. "A review of data center cooling technology, operating conditions and the corresponding low-grade waste heat recovery opportunities." *Renewable and Sustainable Energy Reviews* 31 (2014): 622-638. <https://doi.org/10.1016/j.rser.2013.12.007>
- [41] Kenneth, B. "Heat density trends in data processing, computer systems, and telecommunications equipment." *UpTime Institute, White paper* (2005).